

Design of Pressure-Sensitive Adhesives

E. H. ANDREWS* and T. A. KHAN, *Materials Department, Queen Mary and Westfield College, London E1 4NS, United Kingdom*, P. DREW, *Dow Europe S.A., Bachtobelstrasse 3, 8810 Horgen, Switzerland*, and R. RANCE, *Dow Rheinmuenster Gmbh., Industriestrasse 1, 7587 Rheinmuenster, FRG*

INTRODUCTION

Soft-machine peel testing of pressure-sensitive adhesives (PSAs), in which a spring is inserted between the machine crosshead and the peeling strip, provides much more information about the adhesive characteristics than conventional (hard-machine) tests.¹ When the results are presented as plots of $\log(\text{peeling energy})$ vs. $\log(\text{peeling rate})$, soft-machine data provide a lower bound, a transition rate, and an upper bound, only the last of these being obtained from a hard-machine test. For convenience we shall refer to these three characteristics as the soft-machine "parameters" even though the two bounds are, in fact, curves.

Any method that provides improved characterisation of materials is also able, by the same token, to afford an improved design route for new materials. This is because the process of design involves tracing the effects of compositional changes on performance, and performance in turn depends on the physical characteristics of the product. The better characterised the material, the easier it is to tell whether experimental changes in composition are leading towards the desired performance objectives.

Pressure-sensitive adhesives are typically formulated from one or more polymeric materials to which tackifier resins have been added. Other ingredients may include fillers and plasticisers and the polymeric phase may be uncross-linked or partially crosslinked. The study described in this paper was undertaken to compare some commercial and experimental adhesives as a basis for the design of systems that offer advantages of economics, availability, or novelty.

The methodology followed, therefore, was first to characterise a variety of commercially successful products in terms of the soft-machine test and then to see how their "viable" soft-machine parameters could best be reproduced in the experimental chemical system under investigation. Then the soft-machine parameters (lower bound, upper bound, and transition rate) were determined as functions of the molecular weight, polymer composition, and tackifier level in the experimental adhesives. From the spectrum of parameters thus obtained it was possible to select those experimental polymers that closely matched commercial materials. Different combinations of the compositional variables could be found that matched commercial adhesives intended for different functions (e.g., removeable and permanent tapes). Thus, it was possible to predict what composition in the experimental adhesive system would be best suited for a particular application, on the assumption that if all three soft-machine

parameters matched those of a successful product, then the new adhesive is likely to perform equally well. Obviously, this assumption may sometimes prove false, since there may be important properties that are not reflected in the soft-machine parameters. Equally, however, the assumption is more likely to be true if three parameters are matched than if only one is matched. By providing three parameters, therefore, the soft-machine test is far more valuable to the adhesives designer than conventional peel testing. (We must add the proviso that with some systems it is not always possible to detect a lower bound, though this may result from a lack of sensitivity at very low peeling forces rather than an intrinsic property of such systems. However, the presence or absence of a detectable lower bound is itself added information about the adhesive that is not obtained in conventional testing.)

It has been suggested²⁻⁴ that dynamic mechanical analysis can provide design criteria for PSAs. The idea is that good performance is only obtained if certain dynamic mechanical parameters, such as the temperature of the peak in the loss tangent curve (approximating to T_g) and the elastic and loss moduli, fall within certain ranges. To test this idea, dynamic mechanical spectra were recorded for all the experimental adhesives used in this study.

MATERIALS AND PROCEDURES

The experimental adhesives used in this study were a series of carboxylated styrene-butadiene (SB) latices. The latices were chosen to give a range of pressure-sensitive adhesive properties and to cover a range of molecular weight and of T_g (by varying the styrene/butadiene ratio). Since the polymers were not completely soluble in any solvent, but contained a certain level of gel, it was not possible to measure molecular weights quantitatively. Instead, the molecular weights were assessed from the known polymerisation conditions and the level of chain transfer agent used. A single rosin-based tackifier with a softening point of about 40°C was used throughout. This tackifier was used in 50% (wt/wt) emulsion form.

The waterborne latices, with or without added tackifier, were spread uniformly on water-soaked cotton cloth to give a dry weight of about 360 g/m² and allowed to dry at room temperature for 48 h. Peel strips measuring 20 × 130 mm were cut with the long axis coinciding with the warp direction. This provided a strip that did not stretch significantly during peeling.

Types of commercial adhesive tapes and labels studied are listed in Table I.

TABLE I
Commercial Products Studied

Product	Our code	Type
Removable tape	A	Removable
Masking tape	B	Removable
Permanent label	C	Permanent
Packaging tape	D	Permanent
Office tape	E	Permanent
Office tape	F	Permanent

The model substrate (from which the strip is peeled) was float glass cleaned by washing in water (deionised) and acetone. This provides a rigid substrate unaffected by any mobile species in the adhesive and which permits the adhesive interface to be viewed through the substrate. Peel strips were pressed down firmly on the substrate and left for 5 min before use. Any residual air bubbles at the interface could be seen through the glass and eliminated by further pressure.

SOFT-MACHINE PEEL TESTING

We here review the major features of soft-machine testing. Fuller details will be found in the literature.¹ The experimental arrangement is shown in Figure 1, and a schematic force/time curve in Figure 2. The peeling energy Θ is obtained directly from the peel force P and the width b of the peel strip using the formula

$$\Theta = (P/b)(1 - \cos \phi) \quad (1)$$

where ϕ is the peel angle and the formula assumes that the peeled portion of the strip is inextensible.

The peeling rate \dot{c} is no longer equal to the crosshead speed, as it is for hard-machine testing, but is obtained instead from the slope of the force-time curve. Thus

$$\dot{c} = (dX/dt) - k(dP/dt) \quad (2)$$

where k is the inverse spring constant and X is the vertical position of the crosshead (dX/dt is thus the crosshead speed).

In practice, the output from the load cell is digitised and fed to a microcomputer that calculates $\log \Theta$ and $\log \dot{c}$ and outputs a graph of the former against the latter on a plotter.

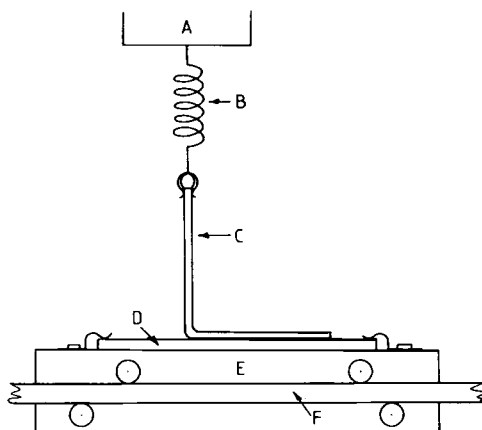


Fig. 1. Soft-machine peel test: (A) crosshead, (B) spring, (C) peel strip, (D) substrate, (E) trolley, (F) bearers.

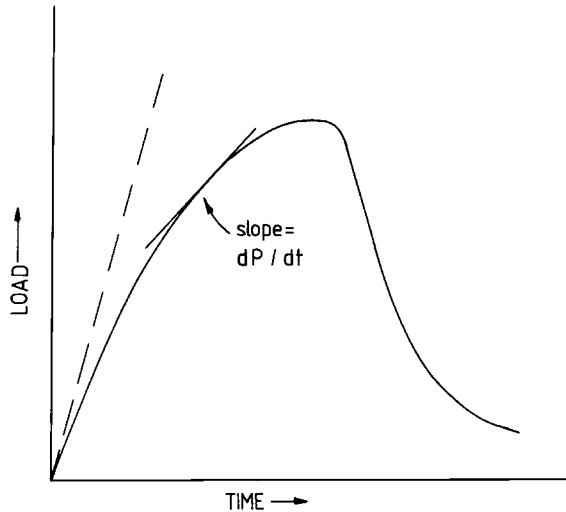


Fig. 2. Schematic load-time trace for a soft-machine peel test. Broken line shows response of spring alone.

It is known⁵ that the adhesive failure energy Θ can be expressed as the product of an intrinsic interfacial energy Θ_0 and a loss function Φ that depends on rate, temperature, and strain, and is a characteristic of the bulk of the adhesive. Thus,

$$\Theta = \Theta_0 \Phi(\dot{c}, T, e) \quad (3)$$

The particular advantage of plotting $\log \Theta$ against $\log \dot{c}$ is that, from (3), the logarithm of Θ is the sum of the logarithms of Θ_0 and Φ , so that changes in Θ_0 at constant Φ result in a vertical shift of the data. It is often possible in this way to separate the effects of interfacial changes from those of bulk changes in the adhesive (which affect Φ but not Θ_0).⁵

A typical soft-machine output is shown in Figure 3 for several different crosshead speeds. At each speed, data are produced over a range of peeling velocities. Taken together the tests therefore define peeling energy over a wide range of peel rates. The upper bound in Figure 3 reproduces the results obtained in hard-machine tests on the same adhesive. The lower bound is a phenomenon only obtained in soft-machine testing, as is the vertical transition from lower to upper bounds. The transition velocity is a function of both the crosshead speed and the spring stiffness, and is not therefore a material property in itself. However, when the transition velocity is plotted against the loading rate dP/dt (which is normally constant during the transition), an initially linear plot is obtained whose slope S is independent of the crosshead speed and spring stiffness. It is the parameter S , therefore, that characterises the adhesive system rather than the transition velocity *per se*. The physical significance of S is discussed below.

The physical significance of the three soft-machine parameters is as follows. Lower bound behaviour arises when peeling occurs without fibrillation of the adhesive. This occurs at very low loads or in crosslinked adhesives that have

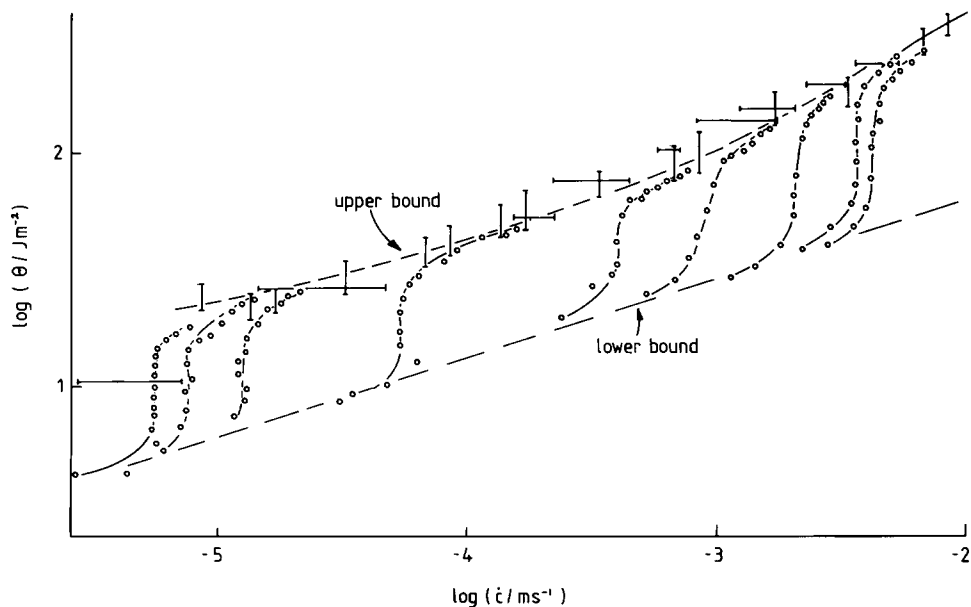


Fig. 3. Soft-machine data (circles), hard-machine data (vertical error bars), and dead-load peeling data (horizontal error bars) for a natural rubber-based surgical adhesive (after ref. 1), showing upper and lower bounds. Each sigmoidal soft-machine curve is obtained at a single crosshead speed, increasing left to right.

insufficient ability to flow (fibrillation requires plastic flow of adhesive since it involves the creation and enlargement of cavities within the material). In freely flowing adhesives the ease of fibrillation may be such that no lower bound is observed, which is fairly common with acrylic PSAs, for example.

The transition involves the progressive thickening of the layer of adhesive actually being fibrillated. This is shown schematically in Figure 4 and can be likened to the process of craze thickening observed in glassy plastics. The transition is initiated by the onset of the "crazing" mechanism (either cavitation⁶ or meniscus instability⁷ at a critical load that is rate and temperature dependent. In Reference 1 preliminary data indicated that, for a given system, the parameter S decreases with increasing temperature and with increasing plasticisation. Results reported in this paper also suggest that S is directly related to the viscosity or flow properties of the adhesive. The dimensions of this parameter are not, of course, those of viscosity and a theoretical connection between S and viscosity has not yet been established. There is, however, mounting evidence that S reflects the flow properties of the adhesive and this is not unreasonable since the parameter relates to the onset of "craze thickening," a process directly related to flow. One of the results of the present study is that the empirical parameter S does, in fact, correlate well with viscous flow data (i.e., shear rates). The upper bound occurs when the capacity for craze thickening is exhausted, which results when the full thickness of the adhesive layer is involved in the fibrillation process. It is for this reason that the upper bound, unlike the lower bound, is strongly dependent on the thickness of the adhesive layer (see Fig. 5).

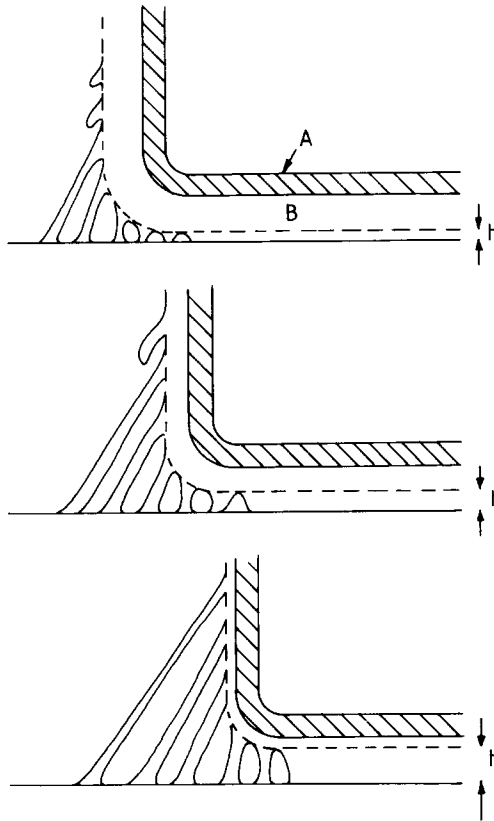


Fig. 4. Schematic showing progressive thickening of the fibrillating layer, h , as peeling proceeds. This process corresponds to the vertical transition region in soft-machine curves such as shown in Fig. 3. (A) backing material, (B) adhesive layer.

EXPERIMENTAL

Peel strips were prepared from the commercial and experimental adhesive systems as already described and subjected to both hard- and soft-machine testing at $23 \pm 3^\circ\text{C}$ and at three crosshead speeds, namely 10, 100, and 500 mm/min using a J&J tensile testing machine in conjunction with a BBC(B) microcomputer. Cast specimens 1 mm thick were also prepared from the adhesives and used, in the shear mode, to measure a dynamic mechanical spectrum by means of the Polymer Laboratories Dynamic Mechanical Thermal Analyser (DMTA).

Shear holding strength was measured at $23 \pm 1^\circ\text{C}$ in a controlled temperature cabinet in the following manner. Strips of coated cloth, similar to those used for peel testing, were cut with dimensions 20×400 mm and allowed to equilibrate in the test chamber at around 10% RH. One end of each strip was stuck down on a clean float glass plate in such a way as to give an overlap (or adhered length) of 20 mm. The plate was mounted so that the unadhered length of the strip hung vertically under an attached load of 1 kg. The plate itself was set at 2° to the vertical to avoid any unintentional peeling action (i.e., the "peel angle" was set at -2°). To determine shear strength, the elapsed time was

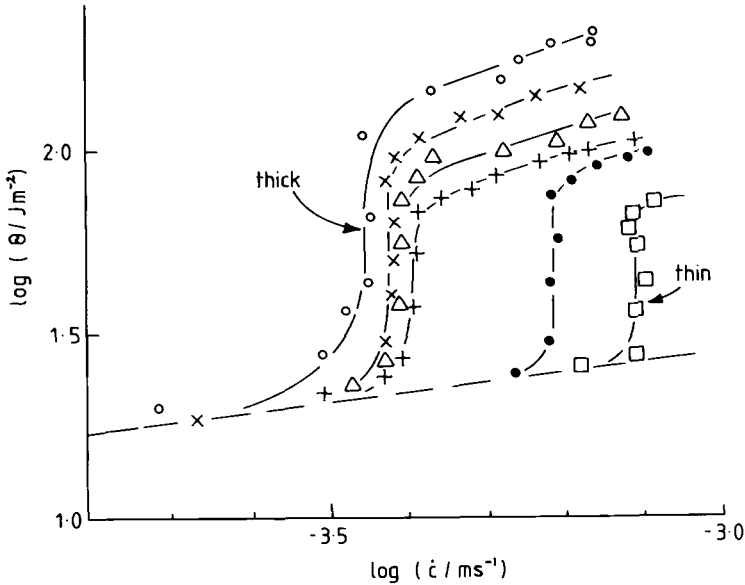


Fig. 5. Effect of adhesive layer thickness on soft-machine peel curves. Adhesive loadings in g/m^2 are (from left to right) 942, 332, 309, 215, 149, and 107.

measured for each 2 mm of sliding. The average shear stress was calculated for each sliding interval, using the current adhesive contact area (which, of course, reduces with time as the strip slides off the glass). The shear displacement (or sliding) rate ds/dt was also calculated.

RESULTS

Commercial Tapes

Results on commercial tapes were limited to soft-machine testing. DMTA specimens could not be prepared from these materials for obvious reasons.

The combined hard- and soft-machine data for the five commercial tapes are shown in Figures 6–11, the hard-machine data being represented always by error bars and the soft-machine data by points. In all the results presented in this paper, open symbols are used to indicate the adhesive failure mode and filled symbols the cohesive mode.

The results for removable tape A (Fig. 6) are particularly interesting in that the upper and lower bounds coincide. Strictly speaking, there is no upper bound since no fibrillation occurs. This is typical of a crosslinked adhesive where plastic flow is prevented and peeling is a simple cleavage process between the adhesive and the substrate. The peeling energy is, consequently, very low at $10\text{--}20 \text{ J}/\text{m}^2$.

In contrast (Fig. 7), masking tape B, another removeable tape, shows the classic behaviour of a PSA, with a lower bound, a transition, and an upper bound. While the lower bound is of the order of $10 \text{ J}/\text{m}^2$ depending on peeling rate, the upper bound is around $600 \text{ J}/\text{m}^2$, 60 times greater. Most of the peeling energy is dissipated in the formation and plastic stretching of filaments. It

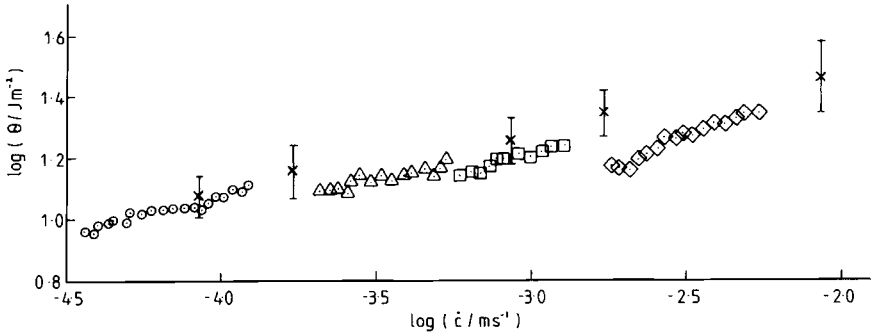


Fig. 6. Soft-machine data (points) and hard-machine data (error bars) for removable tape A. Upper and lower bounds coincide due to crosslinking (no capacity for flow in the adhesive). Cross-head speeds are (from left to right) 10, 100, and 500 mm/min.

appears that removability does not require a nonflowing system, as would at first sight seem necessary.

Permanent label C again displays classical behaviour (Fig. 8), and is very similar to tape B in terms of the three soft-machine parameters. However, there are differences. The logarithmic difference between upper and lower bounds is about 1.6 for tape B but only 1.2 to 1.4 for label C. The latter also displays a tendency for the transition velocity to oscillate between two values, especially at higher speeds. It proved impossible to obtain higher speed peel results with label C because the backing material tore before a steady peeling force was established. This illustrates another advantage of soft-machine testing, since soft-machine data were readily collected under these conditions. The failure of

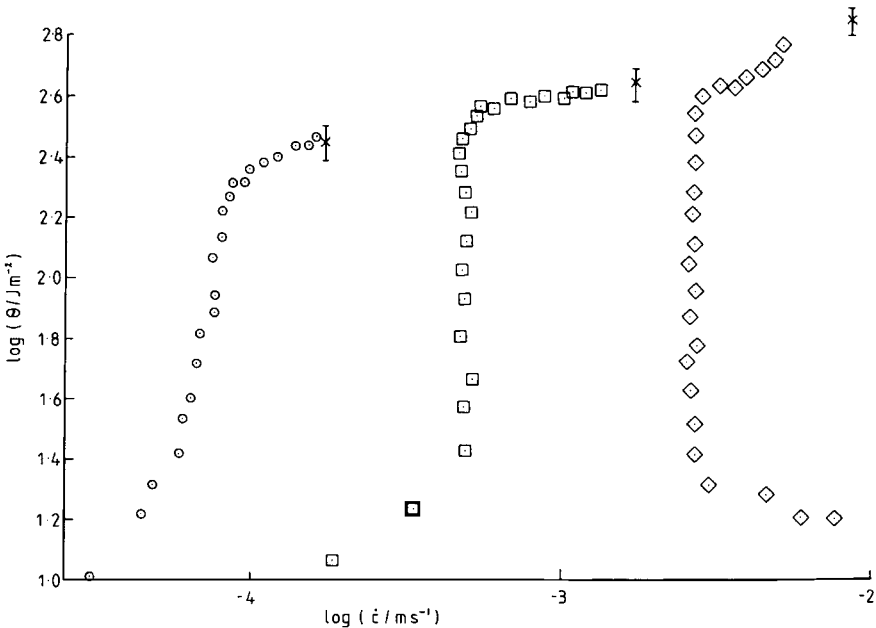


Fig. 7. Soft-machine data (points) and hard-machine data (error bars) for masking tape B.

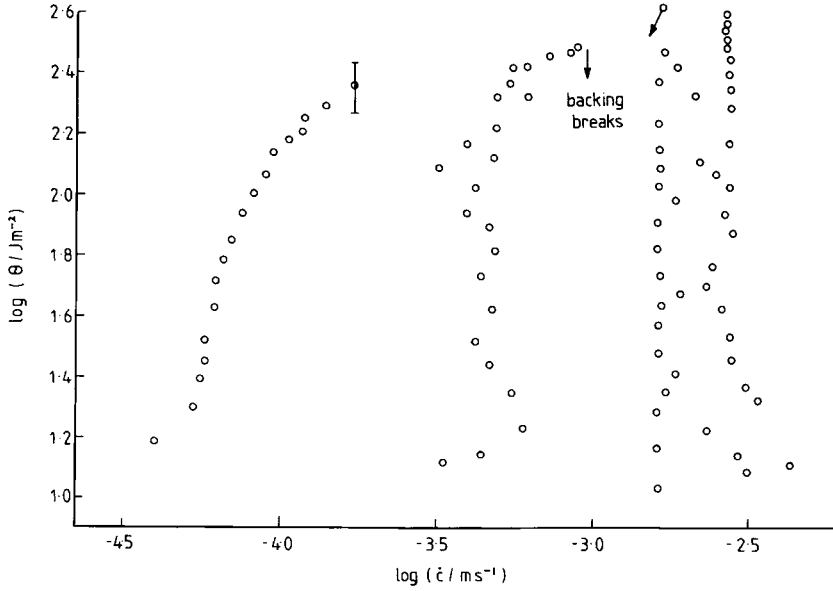


Fig. 8. Soft-machine data (points) and hard-machine data (error bars) for permanent label C.

the backing material, rather than the adhesive behaviour as such, is what makes label C permanent rather than removable.

Packing tape D (Fig. 9) has a significantly lower upper bound than the two previous materials, but the lower bound (as far as can be ascertained) remains around 10 J/m^2 . The transition behaviour is somewhat anomalous, though the oscillation at high speeds and the “C” shape instead of “S” curves are both features seen in other systems as already noted.

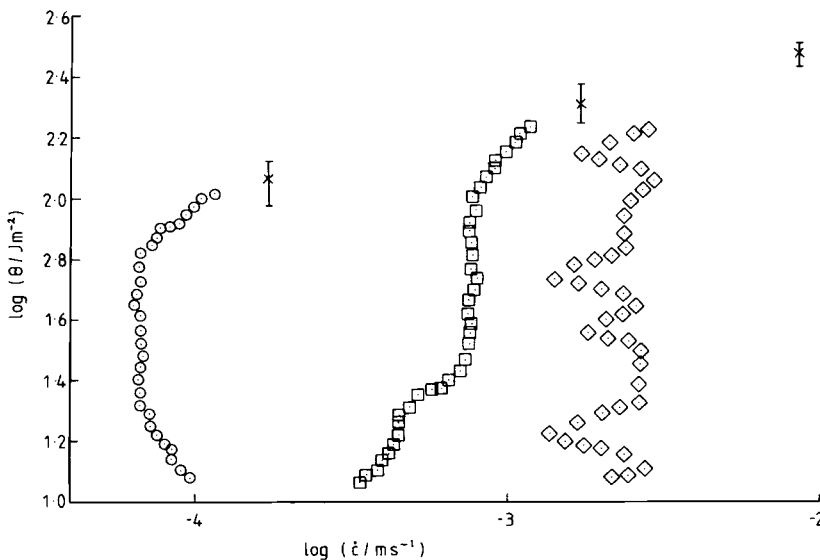


Fig. 9. Soft-machine data (points) and hard-machine data (error bars) for packaging tape D.

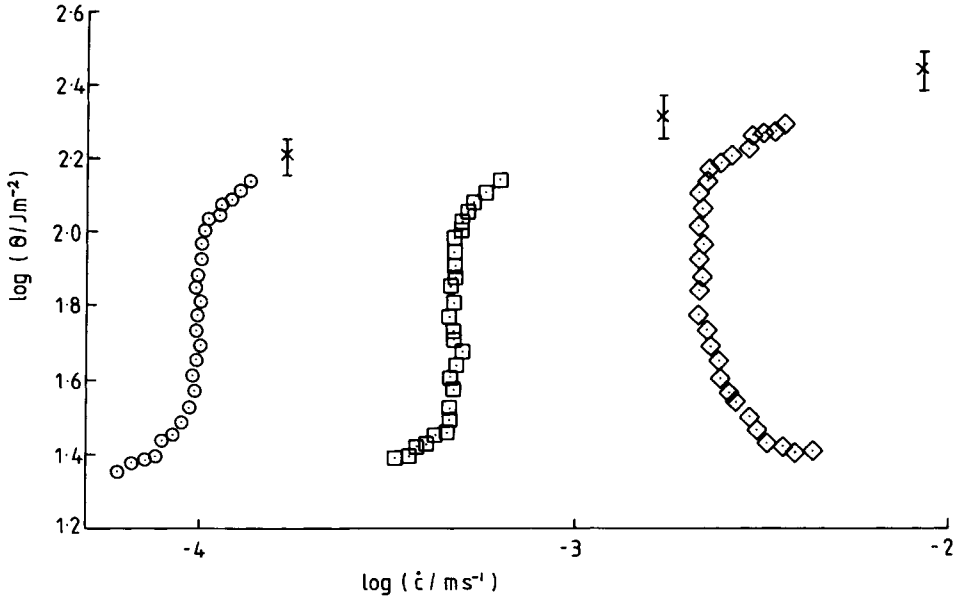


Fig. 10. Soft-machine data (points) and hard-machine data (error bars) for office tape E.

Office tape E (Fig. 10) differs from all previous materials in having a raised lower bound, around $20\text{--}25\text{ J/m}^2$. The upper bound is also relatively low at about $100\text{--}300\text{ J/m}^2$ depending on rate. Both normal "S" shaped and "C" shaped curves are evident, the latter at higher speeds.

Office tape F (Fig. 11) behaves in a manner very similar to office tape E, with similar upper and lower bounds and well-behaved sigmoidal curves.

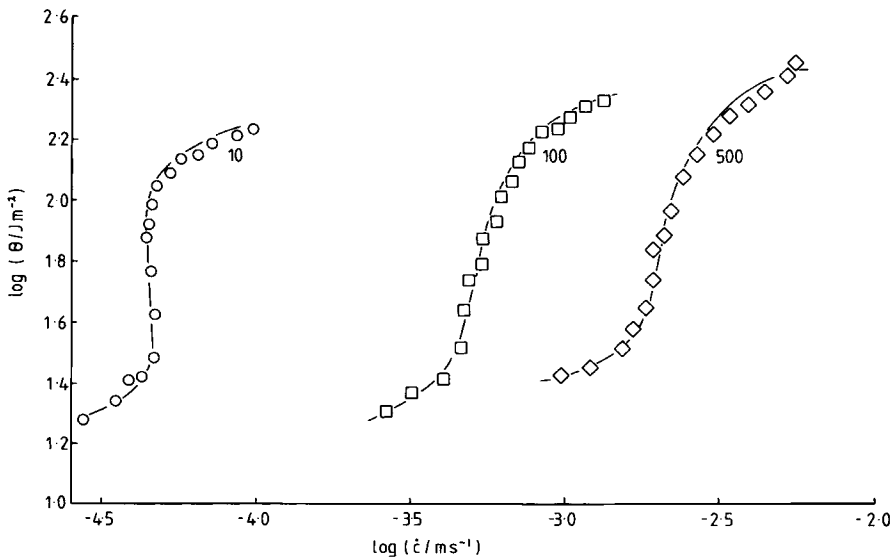


Fig. 11. Soft-machine data (points) and hard-machine data (error bars) for office tape F.

The transition data have been further analysed in terms of the parameter S introduced earlier. Table II shows these values for the six commercial tapes.

As discussed earlier, we believe that this parameter is related to viscosity. Thus, an S value of infinity corresponds to an infinite viscosity and indicates a crosslinked system incapable of flow. Normally, flow can be induced in a PSA if the rate of deformation is sufficiently reduced. An infinite slope on the curve of loading rate vs. transition speed (as obtained for tape A) indicates that, even at infinitely slow rates of peeling, no flow is obtained. Fibrillation therefore never occurs and the material displays only a lower bound. The remaining tapes have S values within the range 72–145 N/m (at 23°C), that is, varying by a factor of about two. This range appears to provide a design criterion for acceptable flow behaviour in PSA systems, although much higher values (to infinity) are acceptable for tapes that are intended for easy removal.

Carboxylated Styrene–Butadiene Adhesives: Peel Data

Three different polymers were used designated by codes H, M, and L, representing high, medium, and low molecular weights, respectively. Polymer H had a higher butadiene content than polymers M and L. Varying levels of tackifier were also used.

The effect of tackifier level was the first matter studied and the results are summarised in Figure 12, which shows upper and lower bounds at a peeling speed of 10 mm/min as functions of tackifier level for the three SB adhesives. It will be seen that the failures were all cohesive (filled symbols) for the low molecular weight polymer L; mostly cohesive for the intermediate molecular weight M; while the high molecular weight material H displayed considerable adhesive failure (open symbols), especially at low tackifier levels. This change from cohesive to adhesive failure is typical of a change from low to high molecular weight and of increasing crosslinking.

Upper bounds all display a maximum at 50% tackifier. The two low BD polymers undergo a collapse of the upper bound as tackifier levels fall below about 35%. This probably reflects the fact that the fall in T_g with decreasing tackifier (see DMTA data below) leaves the material increasingly high above its T_g , and therefore increasingly liquid. In the absence of long molecules and/or crosslinking, rubberlike integrity is not established and the adhesive fails at low elongation (and thus low energy absorption). As tackifier levels increase, T_g rises into the use-temperature range, improving the capacity for energy dissipation and thus maximising the upper bound. Excessive tackifier, however,

TABLE II
Values of the Parameter S for Commercial Tapes

Tape code	S N/m
A	∞
B	145
C	120
D	72
E	111
F	96

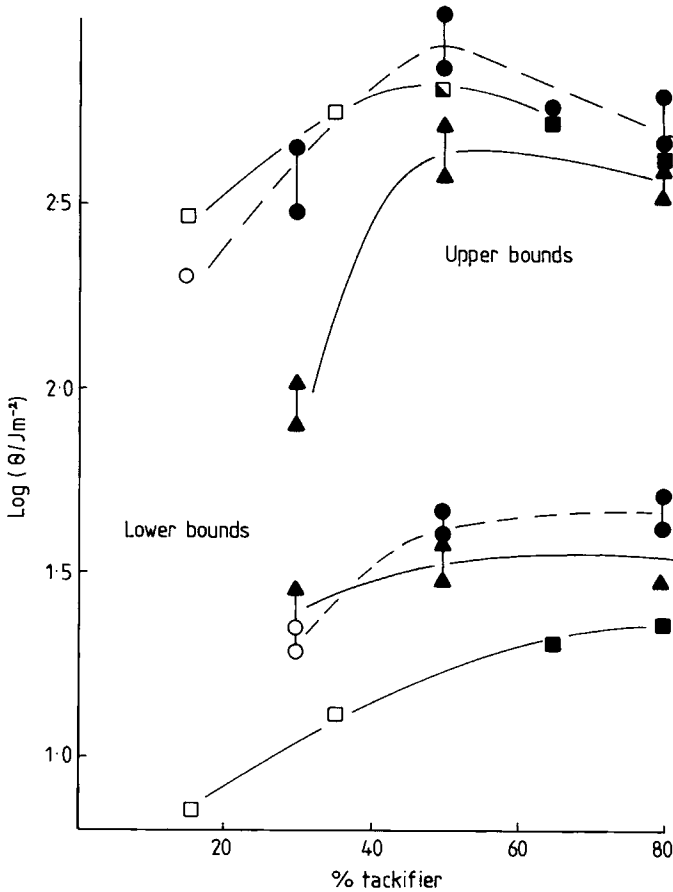


Fig. 12. Upper and lower bounds for three styrene-butadiene experimental resins, at an arbitrary peeling rate of 10 mm/min, as functions of the tackifier content. Filled symbols, cohesive failure; open symbols, adhesive failure. H, squares; M, circles; L, triangles.

also destroys molecular integrity by reducing entanglements and above a certain level the upper bound begins to decline, giving rise to the observed maximum in Figure 12.

The lower bounds also vary systematically with tackifier content, rising as the latter increases but tending to level out above 50% tackifier. The lower bound is significantly lower for the high BD polymer and does seem to correlate with T_g , decreasing slowly as T_g falls (see later). This is consistent with a viscoelastic origin for the lower bound, this being the energy required to drive a simple cleavage crack along the interface without fibrillation ("crazing").

The transition velocity falls progressively as tackifier is added. The plot of loading rate vs. transition velocity is linear up to crosshead speeds of 100 mm/min and the slope S determined for these systems is plotted in Figure 13 against tackifier content. Sigmoidal curves result, showing a greater range of values for the high BD polymer. For comparison, the S values for commercial products are included as short horizontal lines; the polymer type in these products is not known nor are the tackifier contents, if any. Figure 13 shows that the S

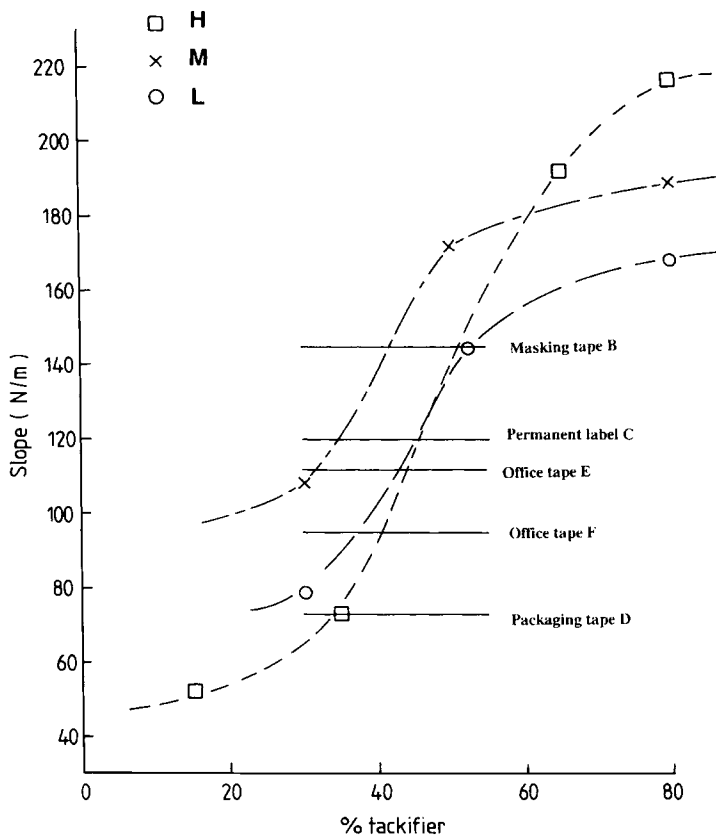


Fig. 13. The slope parameter, S , as a function of tackifier content for the three experimental adhesive resins. H, squares; M, crosses; L, circles. Also shown are the S -values for commercial tapes.

values of the commercial products can be matched by blends of the experimental latexes with 30–50% tackifier.

Within the experimental group, the S values for polymer M are consistently higher than for polymer L, which is consistent with the idea that S rises as viscosity increases. At high tackifier content, polymer H also falls in sequence, but at low tackifier actually has a lower S than the lower molecular weight materials. It must be remembered, however, that polymer H has a different composition (higher BD content) and thus a lower T_g at a given tackifier level. Tests at room temperature therefore find this polymer relatively further above T_g than the others and thus, presumably, more fluid. At high tackifier content the higher molecular weight of H predominates by sustaining entanglements, producing greater viscosity than M and L in spite of the T_g effect.

Finally, the rise of S with tackifier can be understood directly in terms of the rising T_g as tackifier is added. This is rheologically equivalent to reducing temperature, and viscosity (and thus S) increases as expected.

Shear Holding Results

The instantaneous average shear stress, $\bar{\tau}$, was plotted against the sliding rate, ds/dt , and Figure 14 shows typical results. The curve consists of two

regions. In the first, a threshold shear stress is required to produce any sliding and then a linear plot is obtained, the slope of which we shall designate q . At some point the shear stress begins to increase rapidly because of the diminishing area of contact, but the sliding rate does not increase proportionately. Thus, the curve in Figure 14 displays an upturn. (Note: In some systems to be described in a further paper, the upturn is preceded by a large increase in sliding rate corresponding to a jump along the sliding-rate axis.)

Region two of the curve occupies most of the lifetime of the test and has been chosen to characterise the shear holding behaviour. In particular, the slope q in this region will be used as an appropriate parameter. The lower this slope, the lower is the apparent viscosity of the adhesive. Indeed, if the sliding rate were divided by the adhesive layer thickness to give a shear rate, the slope would be the apparent Newtonian viscosity. This was not done, however, since the thickness dependence is far greater than can be accounted for by such simple considerations. All q data used were measured at a constant adhesive loading of 36 mg/cm^2 to overcome the problem of thickness dependence.

Figure 15 shows a plot of $\log q$ against S , the transition parameter derived from the soft-machine peel data. A logarithmic scale was required for q because of its large variation between materials. An excellent correlation is obtained for the three experimental polymers at various degrees of tackification. This clearly vindicates the idea that the S parameter from soft-machine testing characterises the adhesive's capacity for flow. High S and high q alike correspond to high viscosity. However, it will require a thorough analysis of the shear holding test to determine the precise significance of these parameters. In particular, it is clear that q varies much more rapidly than S as the viscosity changes from one material to another.

Dynamic Mechanical Data

Finally, for the carboxylated SB adhesives, we may consider the DMTA data and whether they correlate with the soft-machine data in any way. A summary

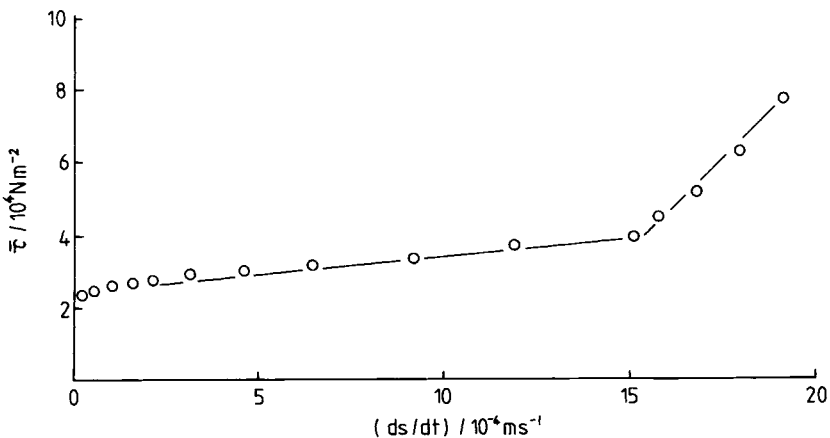


Fig. 14. Typical shear holding data for one of the experimental adhesives, shown as a plot of nominal shear stress against sliding rate.

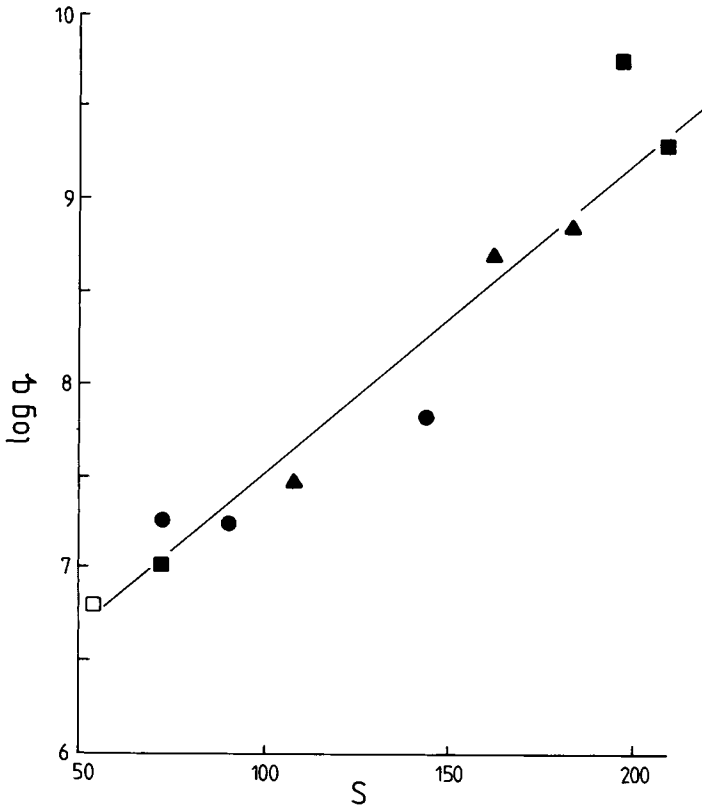


Fig. 15. Correlation between the parameter q from shear holding tests and the parameter S from soft-machine peel tests for three experimental resins at various tackifier levels.

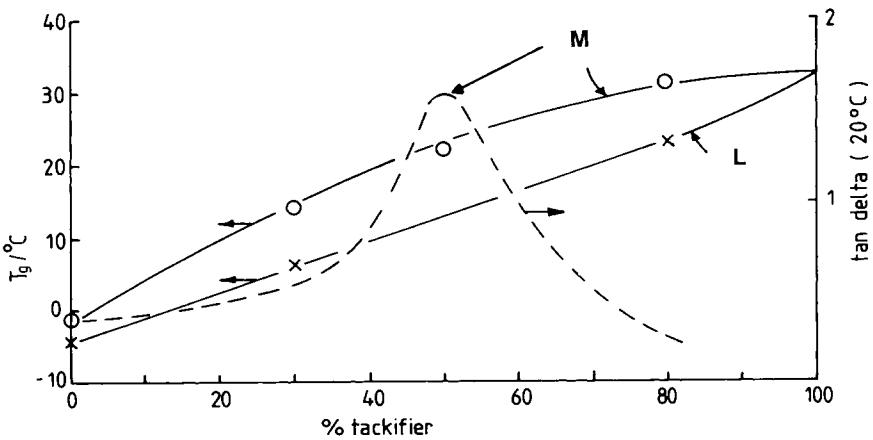


Fig. 16. Dependence of dynamic mechanical data upon tackifier content for some of the experimental resins. M, circles and broken line; L, "x".

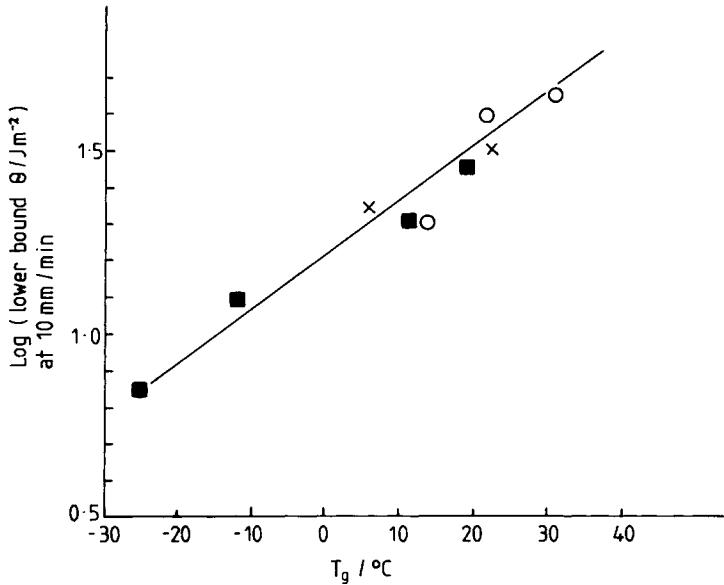


Fig. 17. Correlation of lower bound with glass transition temperature for the experimental resins at various tackifier levels.

of the DMTA results for two of the experimental resins is given in Figure 16. This shows the variation in apparent T_g (i.e., the temperature of the peak in the $\tan \delta$ curve), and in $\tan \delta$ itself (at 20°C), with tackifier content. The heating rate was $5^\circ\text{C}/\text{min}$ and the frequency of test was 1 Hz.

As expected, the glass transition rises smoothly with the addition of tackifier for both materials. $\tan \delta$ (20°C) rises to a peak at 50% tackifier content, this being the composition that gives a $\tan \delta$ peak in the region of 20°C . Comparing the $\tan \delta$ vs. tackifier curve with the plot of upper bound against the same variable (Fig. 12) suggests a correlation, namely that the upper bound follows

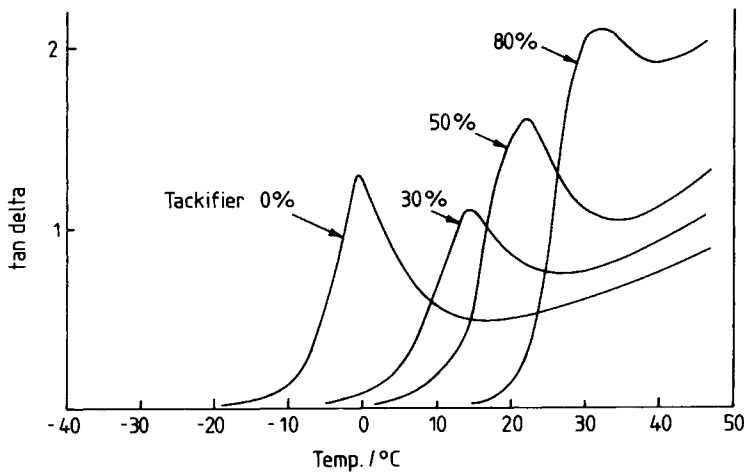


Fig. 18. Effect of tackifier level on the shape of the $\tan \delta$ curve for the latex M.

$\tan \delta$. This is not unexpected, since both upper bound and $\tan \delta$ reflect the capacity of the adhesive to dissipate energy.

However, the correlation is not simple, the upper bound at 80% tackifier being higher than at 30%, whereas $\tan \delta$ is lower at 80% than at 30%. Again, this is not surprising since $\tan \delta$ is a small-strain parameter while the upper bound involves large deformations with substantial flow and leading to fracture.

One would, in fact, expect a closer correlation between the lower bound and $\tan \delta$, since the lower bound does not involve the formation of highly strained filaments. The lower bound, however, does not display a maximum but rather a plateau above 50% tackifier. A correlation does exist between the lower bound and the T_g s of these polymers. This is illustrated in Figure 17, where the lower bound (at an arbitrary peeling speed of 10 mm/min) is plotted against T_g and reveals a good linear relationship for the three polymers at various levels of tackifier. This seems to indicate clearly that the lower bound has a viscoelastic origin.

A further feature of the DMTA curves is the behaviour of $\tan \delta$ above the peak. As the tackifier content is increased, the drop in $\tan \delta$ above the peak diminishes, reflecting an increased propensity for flow above T_g . This is illustrated in Figure 18.

Our present feeling about DMTA data on PSAs is that they are more useful in characterising the adhesives as materials than in providing predictive information or design criteria on adhesive performance. The correlation obtained in Figure 17 does indicate, however, that there is some basis for the idea that DMTA data reflect certain aspects of peel behaviour, though not all. It should particularly be noted that the interfacial parameter Θ_0 in eq. (3) cannot, by definition, be reflected in DMTA results since it is not a property of the bulk adhesive but only of the interface with the substrate.

The authors thank the Dow Chemical Company for financial support and for permission to publish this paper, and the Science and Engineering Research Council for a grant in partial support of this research.

References

1. E. H. Andrews, T. A. Khan, and H. A. Majid, *J. Mater. Sci.*, **20**, 3621 (1985).
2. J. B. Class and S. Chu, *J. Appl. Polym. Sci.*, **30**, 805 (1985).
3. J. B. Class and S. Chu, *J. Appl. Polym. Sci.*, **30**, 815 (1985).
4. J. B. Class and S. Chu, *J. Appl. Polym. Sci.*, **30**, 823 (1985).
5. E. H. Andrews and A. J. Kinloch, *Proc. Roy. Soc. (Lond.) A*, **332**, 385 (1973).
6. E. H. Andrews and L. Bevan, *Polymer*, **13**, 337 (1972).
7. A. S. Argon and M. M. Salama, *Phil. Mag.*, **35**, 1217 (1977).

Received March 21, 1989

Accepted September 26, 1989